Progress In Electromagnetics Research Letters, Vol. 61, 31–38, 2016

A Circularly-Polarized Microstrip Antenna with Quad-Band Combination

Wei Wang, Mengjiang Xing*, and Xuyue Guo

Abstract—In this paper, a novel quad-band combination of circularly-polarized microstrip antenna is proposed. This antenna has multi-frequency and quad-polarization with multiple coaxial probes, which cover four bands of the BeiDou navigation system (BDS), meeting different application requirements. By using a stacked structure to achieve feed and using symmetrical slotted method to place the coaxial probes, the multi-frequency antenna is connected together through the middle co-aperture. Meanwhile, the feed position and size are constantly optimized until get the most suitable one, and the necessary perturbation is obtained. We also introduce a broadband stripline 90° bridge. Ultimately, the circularly-polarized and multi-frequency operation is achieved. Furthermore, the novel design enables easy implementation, miniaturization, wide band, which can meet the application requirements and promote the development of the BDS, which can be combined with the Internet of Things technology, applied to life and production.

1. INTRODUCTION

The BDS is created by China's independent research and development, which is the world's fourth largest navigation system, and other three are the United States Global Positioning System (GPS), the Russian "GLONASS" system, the European "Galileo" system, which are more mature [1–5]. Due to different working environments and carriers, a navigation system must be equipped with different combinations of different properties of a circularly-polarized antenna, to get better wireless communication performance and applications [6]. The BDS plays an important role in both military and civilian fields. The BeiDou antenna as an essential part of the satellite communications decides information receiving and sending [7]. Based on the first and second generations of the BDS, the Beidou antenna can be used to solve the problem of poor isolation of a multi-frequency antenna layer [8, 9], which is suitable for space, vehicle and ship navigation and other equipment [10–12].

In recent years, the BDS is developing rapidly, especially with the BDS to enter the global networking phase, is expected to be completed in 2018 [13]. Based on the research of multi-frequency and multi-polarization of the BeiDou antenna, Li et al. establish a common-aperture and tri-band tri-polarized microstrip antenna, from Chongqing University of Posts and Telecommunications, Research Center for Application of New Communication Technologies [14]. The satellite navigation terminal is also studied, which can receive signals from other satellite navigation systems. Song et al. design an antenna for the BeiDou multi-band microstirp navigation system, from Antenna Servo Professional Unit, the 54th Research Institute of CETC [15]. The multi-band microstrip antenna for GPS L1, GLONASS and BDS is designed [16, 17]. By the use of stack structure, multi-band operation is achieved. According to the Beidou antenna design above, for meeting the use of the multi-bands and different bands for different purposes, this paper proposes a novel design of multi-band circularly-polarized

Received 28 January 2015, Accepted 7 June 2016, Scheduled 24 June 2016
* Corresponding author: Mengjiang Xing (hfssmodel@163.com).
The authors are with the School of Faculty of Information Engineering and Automation, Kunming University of Science and Technology, Kunming, China.

antenna [18, 19], which has strong anti-interference ability, and the development and application of multi-frequency antennas are further promoted.

The antenna schematic is as shown in Fig. 1. The frequency range of B3 is 1250.618–1286.432 MHZ, frequency range of S 2482–2497 MHZ, frequency range of B1 1559.052–1591.788 MHZ, and all of them are the downlink frequency bands. The frequency range of L is 1611.6–1621.76 MHz, which is the uplink frequency band. The four bands can work independently and play their respective functions. After the LNA (Low Noise Amplifier) and filter, the received signal turns into the desired signal, then through the RFA (Raman Fiber Amplifier), Mixer, IF filter, AGC (Automatic Gain Control), ADC (Analog-to-Digital Converter) outputs the signal to the specified device. PLL provides the local oscillator frequency to adjust the circuit. The path of the transmitted signal L is opposite to the path of the received signal B3, B1, and S [20].

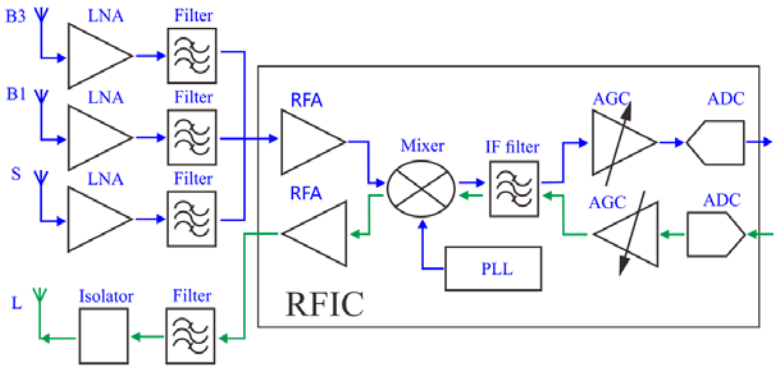

Figure 1. The schematic of the antenna.

2. ANTENNA DESIGN

According to the requirements of the satellite navigation system, BeiDou satellite navigation system has a short message function and positioning function. The antenna has the function of the short message, and its polarization mode is left-handed circular polarization. The center frequency of the transmitting antenna is 1616 MHZ, and the center frequency of the receiving antenna is 2492 MHZ. The antenna has the positioning function as the receiving antenna, in which downward polarization mode is right-handed circular polarization, and the center frequency is 1268 MHZ and 1561 MHZ.

2.1. Parameter Settings

The design method of the square patch is used according to the equations of rectangular microstrip patch. The approximate equation about the size of the patch is as follows [21]:

$$L = \frac{c}{2f_0\sqrt{\varepsilon_r}} \tag{1}$$

In the above equation, L is the physical length of the silver patch, c the speed of light in free space, ε_r the dielectric constant of dielectric plate, and f_0 the resonant frequency of the patch. According to the above equation, the center coordinate position of the feed probe can be initially determined by $X = Y = 0.15L$ [21].

2.2. Antenna Structure

In the antenna structure shown in Fig. 2, there are five dielectric plates in dark gray, and their parameters are $a = 75\,\text{mm}$, $b = 65\,\text{mm}$, $c = 45\,\text{mm}$, $d_1 = 3.5\,\text{mm}$, $d_2 = 2\,\text{mm}$, and $d_3 = 0.5\,\text{mm}$. The materials of the third layer of the dielectric plate with the relative permittivity $\varepsilon_r = 6.0$ and the materials of the other layer with the relative permittivity $\varepsilon_r = 2.65$. There are five silver patches in orange, and

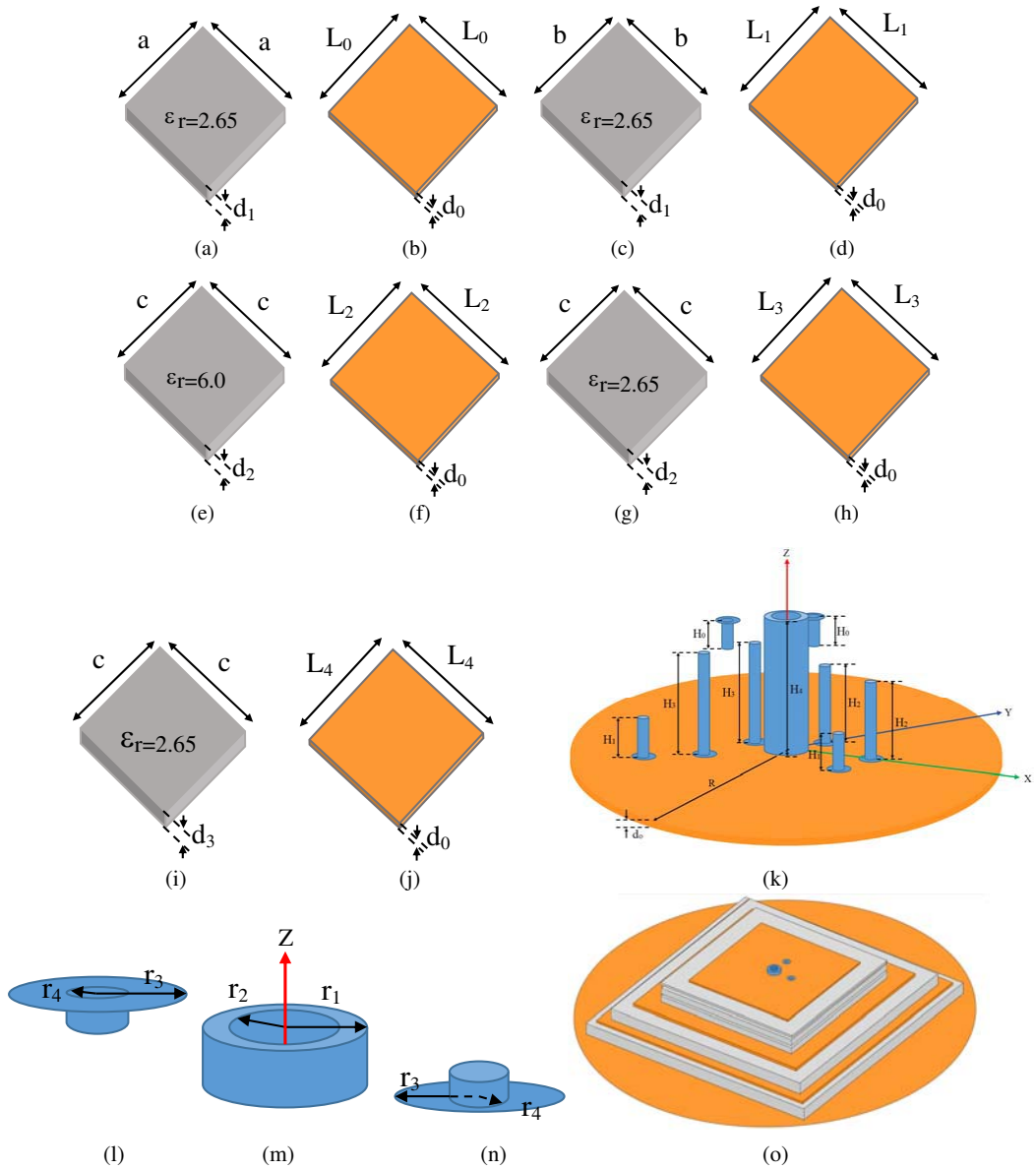

Figure 2. Geometry of the proposed antenna. (a) (c) (e) (g) (i) are the dielectric plates; (b) (d) (f) (h) (j) are the silver patches; (k) (l) (m) (n) are the feed probes; (o) the 3D structure.

their parameter are $L_0 = 70.85\,\text{mm}$, $L_1 = 56.35\,\text{mm}$, $L_2 = 37.1\,\text{mm}$, $L_3 = 35.1\,\text{mm}$, $L_4 = 34\,\text{mm}$, and $d_0 = 0.01\,\text{mm}$. The patches/plates are stacked in sequence in the antenna structure. Firstly, place (a), and then (b) is placed over the top of the (a). Secondly, (c) is placed over the top of (b). Thirdly, (d) is placed over the top of (c), according to this law. From the bottom to the top are (a), (b), (c), (d), (e), (f), (g), (h), (i), (j). The positions of the feed probes as shown in Figs. 2(k), (l), (m), (n), and their parameters are H_0 =2.52 mm, $H_1 = 3.51\,\text{mm}$, $H_2 = 7.02\,\text{mm}$, $H_3 = 9.03\,\text{mm}$, $H_4 = 12.56\,\text{mm}$, $R = 73\,\text{mm}$, $d_0 = 0.01\,\text{mm}$, $r_1 = 2\,\text{mm}$, $r_2 = 1.25\,\text{mm}$, $r_3 = 1.15\,\text{mm}$, $r_4 = 0.5\,\text{mm}$. (l), (m) and (n) are the enlarged parts of the part of (k) for the convenience of marking. The probe's name is named after the name of the height. The center coordinates of H_0 are (0 mm, 5.8 mm, 9.03 mm) and (−5.8 mm, 0 mm, 9.03 mm), connecting to (f), controlling the implementation of S by adjusting its position. The center coordinates of H_1 are (−9.5 mm, −9.5 mm, −0.01 mm) and (9.5 mm, −9.5 mm, −0.01 mm), connecting to (b), controlling the implementation of B3 by adjusting its position. The center coordinates of H_2 are (0 mm, 8.2 mm, −0.01 mm) and (8.2 mm, 0 mm, −0.01 mm), connecting to

(d), controlling the implementation of B1 by adjusting its position. The center coordinates of H_3 are (-5.5 mm, -5.5 mm, -0.01 mm) and (-5.5 mm, 5.5 mm, -0.01 mm), connecting to (f), controlling the implementation of L by adjusting its position. The center coordinates of H_4 and the largest cylinder are (0 mm, 0 mm, -0.01 mm). The largest cylinder is ground plate. The dielectric plates and patches are connected together through H_4 that is the middle co-aperture by the broadband stripline 90° bridge, which connects to the ground plate. Finally, the 3D structure is shown in Fig. 2(o). Each patch achieves circular polarization band coupled with the feed probes in symmetrical positions. By constantly adjusting the size of the patch, position and radius of the probe, the antenna achieves circular polarization at the resonant point.

3. SIMULATION AND EXPERIMENTAL ANALYSIS

After the simulation and optimization by using the HFSS15.0, various parameters are constantly adjusted and relatively satisfied results obtained through analysis and simulation study. Then according to the antenna models, physical antenna is made and measured, as shown in Fig. 3. Its height is 32 mm, and radius is 73 mm. The Agilent8753ES network analyzer is used to verify the validity and accuracy of the results. Due to the actual experimental conditions, only the S parameters of the physical antenna are measured.

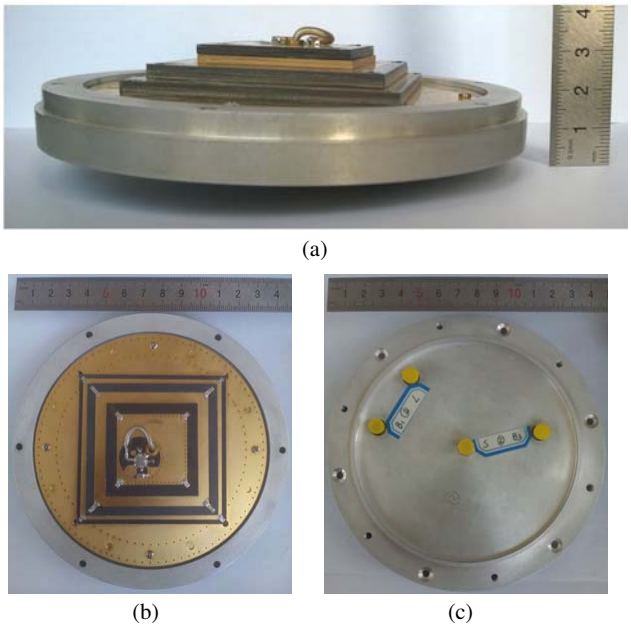

Figure 3. Photograph of the proposed antenna, (a) front view, (b) top view, (c) back view.

3.1. S_{11} Parameters

The simulation and measurement results are shown in Fig. 4. The frequency of 1268 MHZ is shown in Fig. 4(a). The simulation result shows that the impedance bandwidth of VSWR $\leq$ 2 is 26 MHZ (approximately 2.05%) and returning loss $m_1 = -25.60$ dB. The measurement result shows that the impedance bandwidth of VSWR $\leq$ 2 is 55 MHZ (approximately 4.30%) and returning loss $m_2 = -20$ dB. The frequency of 1561 MHZ is shown in Fig. 4(b). The simulation result shows that the impedance bandwidth of VSWR $\leq$ 2 is 10 MHZ (approximately 0.64%) and returning loss $m_3 = -12.075$ dB. The measurement result shows that the impedance bandwidth of VSWR $\leq$ 2 is 7.5 MHZ (approximately 0.48%) and returning loss $m_4 = -24.510$ dB. The frequency of 1616 MHZ is shown in Fig. 4(c). The simulation result shows that the impedance bandwidth of VSWR $\leq$ 2 is 32 MHZ (approximately 1.98%) and returning loss $m_5 = -19.46$ dB. The measurement result shows that the impedance bandwidth of VSWR $\leq$ 2 is 46 MHZ (approximately 2.85%) and returning loss $m_6 = -8.642$ dB. The frequency

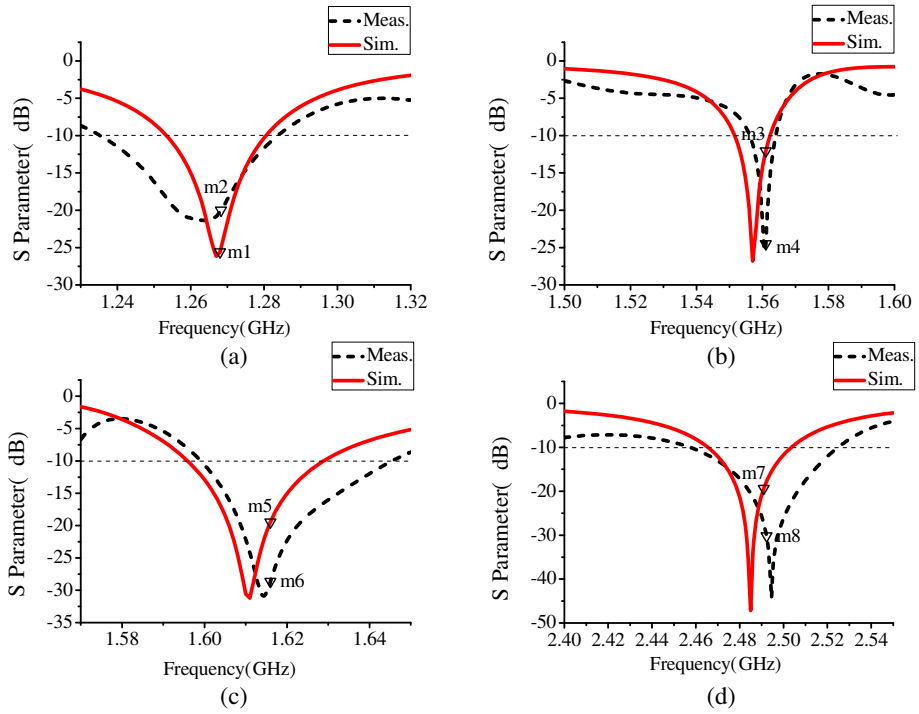

Figure 4. The simulated and the measurement S_{11} parameters of the proposed antenna at four frequency bands, (a) the result of B3, (b) the result of B1, (c) the result of L, (d) the result of S.

of 2492 MHZ is shown in Fig. 4(d). The simulation result shows that the impedance bandwidth of VSWR ≤ 2 is 37 MHZ (approximately 1.48%) and returning loss $m_7 = -18.063$ dB. The measurement result shows that the impedance bandwidth of VSWR ≤ 2 is 38 MHZ (approximately 1.53%) and returning loss $m_8 = -20$ dB.

Overall, the measurement results are better than the simulation ones, in addition to B1. The simulation results are obtained in a relatively ideal environment, but there are many interference factors in the measurement process. The data result is measured in the frequency range of the four bands. For the BeiDou system, the impedance bandwidth of the frequency band above meets the design requirements [13]. The measurement result becomes worse due to the machining accuracy. Because of the processing technology, the frequency point of the simulation curve is on the right side of the lowest point, but the frequency point of the physical antenna will fall near the lowest point. Due to the processing operations, the instability of relative permittivity, instability of material, influence of test environment, etc., the final measured result has a slight deviation, which is acceptable. The measured results basically tallies with the simulation ones by simple verification. The matching effect between the antenna and the feeder is good, which basically meets the requirements of design and application [12].

3.2. Radiation Pattern

Fig. 5 shows the simulated radiation patterns of the LHCP and RHCP in $\varphi = 0°$. At the center frequency of 1268 MHZ, the RHCP level is greater than the LHCP level 38.8484 dB that is the polarization isolation at the direction of $\varphi = 0°$, and the realized gain of RHCP is -2.4505 dB at the elevation 20° and 2.6492 dB at the elevation 50°. The polarization front-to-rear ratio is 43.6729 dB. At the center frequency of 1561 MHZ, RHCP level is greater than LHCP level 31.5354 dB at the direction of $\varphi = 0°$, and realized gains of RHCP are -1.3811 dB at the elevation 20° and 4.2950 dB at the elevation 50°. The polarization front-to-rear ratio is 42.9109 dB. At the center frequency of 1616 MHZ, the LHCP level is greater than the RHCP level 43.2316 dB at the direction of $\varphi = 0°$, and the realized gain of LHCP is -1.7300 dB at the elevation 20° and -3.7039 dB at the elevation 50°. The polarization front-to-rear

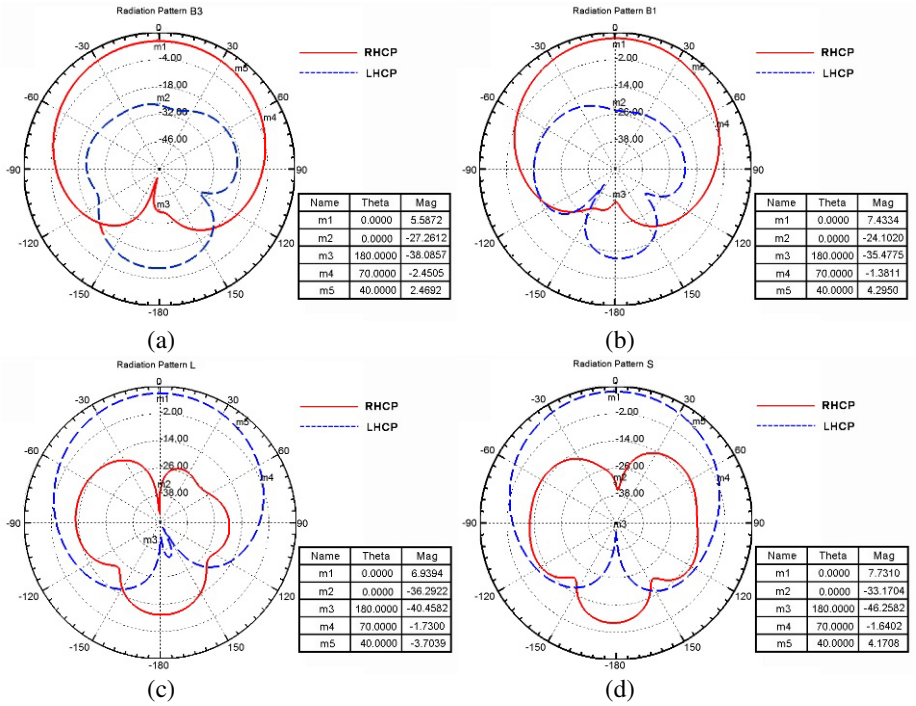

Figure 5. Antenna radiation pattern of the four frequency bands, (a) at 1268 MHZ, (b) at 1561 MHZ, (c) at 1616 MHZ, (d) at 2492 MHZ.

ratio is 47.3976 dB. At the center frequency of 2492 MHZ, the LHCP level is greater than the RHCP level 40.9014 dB at the direction of $\varphi = 0°$, and realized gain of LHCP is -1.6402 dB at the elevation 20° and 4.1708 dB at the elevation 50°. The polarization front-to-rear ratio is 53.9892 dB. The antenna has right-circular polarization at 1268 MHZ and 1561 MHZ, and left-circular polarization at 1616 MHZ and 2492 MHZ. The polarization front-to-rear ratio and polarization isolation are both more than 30 dB, so the antenna has a strong ability to suppress cross polarization and interference.

4. CONCLUSION

In this paper, a novel quad-band combination of circularly-polarized microstrip antenna is designed, providing a wider range of frequency bands. The BeiDou antenna structure realizes circular polarization with different rotation directions by feeding. According to the simulation results, the impedance bandwidth, return loss and radiation patterns all meet the requirement. The Beidou navigation positioning signal is received by the downlink antenna. After RFIC circuits of signal processing, the positioning signals is into the decoder chip, which carries on the analysis to the positioning signal in real time, and then the positioning signal is passed to the embedded chip to display the real-time positioning signals on the LCD (liquid crystal display) screen. The transmit signal is processed by the RFIC circuits, then the uplink antenna transmits the signal, which is received by a particular device, determining that the signal is emitted after a series of circuit processing. Compared to the previously presented work by others, the antenna has good feasibility and practicability, realizing the signal receiving and sending of the BDS, being better applied to the DBS. The four frequency bands can work simultaneously to achieve their own functions, which have more extensive application compared to three frequency bands. The antenna adopts stacked structure to realize the integration of the BeiDou antenna, which has the advantages of low cost, wide frequency band, better miniaturization, and wide application, etc., making it easy to use. Furthermore, this antenna is able to achieve a quad-band antenna compass, which can also achieve good radiation characteristic and circular polarization functions. At the same time it can better achieve antenna miniaturization and broaden the bandwidth of the microstrip antenna.

ACKNOWLEDGMENT

This work was supported by the Fund for Talents of Yunnan Province, China (Grant No. KKSY201403006) and the National Natural Science Foundation of China (No. 61564005).

REFERENCES

1. Lassiter, E. M., "Navstar global positioning system: a satellite based microwave navigation system," *1975 IEEE-MTT-S International Microwave Symposium*, 334–334, 1975.
2. Yonezawa, K., "Evaluation of Geometric Performance of Global Positioning System," *IEEE Transactions on Aerospace and Electronic Systems*, Vol. 14, No. 3, 533–539, 1978.
3. Dale, S. A. and P. Daly, "The Soviet Union's GLONASSs navigation satellites," *Aerospace and Electronic Systems Magazine, IEEE*, Vol. 2, No. 5, 13–17, 1987.
4. Dale, S. A. and P. Daly, "Developments in interpretation of the GLONASS navigation satellite," *Proceedings of the IEEE 1988 National Aerospace and Electronics Conference, 1988. NAECON 1988*, 292–297, 1988.
5. Hu, H. and C. Yuan, "Performance analysis of galileo global position system," *2009 2nd International Conference on Power Electronics and Intelligent Transportation System (PEITS)*, Vol. 1, 396–399, 2009.
6. Chamberlain, S. M., "Combined GPS/GLONASS navigation," *NTC '91., National Telesystems Conference, Proceedings*, 205–210, 1991.
7. "IEEE standard for definitions of terms for antennas," *IEEE Std 145-2013 (Revision of IEEE Std 145-1993)*, 1–50, 2014.
8. Chen, C. and X. Zhang, "Simulation analysis of positioning performance of BeiDou-2 satellite navigation system," *2010 2nd International Conference on Advanced Computer Control (ICACC)*, Vol. 4, 148–152, 2010.
9. Chen, J.-C., D.-J. Zhang, and X.-H. Gao, "Research of BeiDou system in electric power system time service," *China International Conference on Electricity Distribution, 2008. CICED 2008*, 1–5, 2008.
10. Schulze, R., R. E. Wallis, R. K. Stilwell, and W. Cheng, "Enabling antenna systems for extreme deep-space mission applications," *Proceedings of the IEEE*, Vol. 95, No. 10, 1976–1985, 2007.
11. Lu, X., Y. Liao, B. Li, and L. Deng, "BeiDou integrated disaster reduction application platform," *Communications, China*, Vol. 12, No. 8, 169–182, 2015.
12. Hu, Q. and M. Zhang, "Design of positioning and sensing network system based on BeiDou," *2014 International Conference on Wireless Communication and Sensor Network (WCSN)*, 101–105, 2014.
13. Li, J., J. Zhang, B. Zhang, and B. Shen, "Operation and development of beidou navigation satellite system," *2015 International Association of Institutes of Navigation World Congress (IAIN)*, 1–6, 2015.
14. Li, X., F. Wei, and D. Zhang, "A new design of common-aperture and tri-band tri-polarized microstrip antennas," *Chinese Journal of Electron Devices*, Vol. 38, No. 2, 250–253, 2015.
15. Song, Y., L. Liu, and G. Han, "Antenna design for the BeiDou multiband microstrip navigation system," *Electronic Sic. & Apr.*, Vol. 26, No. 4, 137–139, 2013.
16. Li, S., J. Li, X. Gu, H. Wang, C. Li, J. Wu, and M. Tang, "Reconfigurable all-band RF CMOS transceiver for GPS/GLONASS/Galileo/BeiDou with digitally assisted calibration," *IEEE Transactions on Very Large Scale Integration (VLSI) Systems*, Vol. 23, No. 9, 1814–1827, 2015.
17. Li, X., G. Dick, C. Lu, M. Ge, T. Nilsson, T. Ning, J. Wickert, and H. Schuh, "Multi-GNSS meteorology: Real-time retrieving of atmospheric water vapor from BeiDou, Galileo, GLONASS, and GPS observations," *IEEE Transactions on Geoscience and Remote Sensing*, Vol. 53, No. 12, 6385–6393, 2015.

18. Liu, Z., S. Fang, S. Zhu, D. Chen, J. Cao, L. Fu, and Y. Luo, "BeiDou navigation terminal multi-mode asymmetric slots circularly polarized microstrip antenna," *2014 3rd Asia-Pacific Conference on Antennas and Propagation (APCAP)*, 382–385, 2014.
19. Chu, Q., W. Lin, W. Lin, and S. Du, "Broadband quadrifilar helix antenna with compact feeding network," *Acta Electronica Sinica*, Vol. 41, No.4, 722–726, 2013.
20. Zhang, J., "Beidou satellite navigation RF receiver chip of IF Band-pass filter," Xidian University, 2014.
21. Xu, X., *RF Simulation Design Examples by HFSS*, Beijing Electron Industry Press, Beijing, 2015.